

**ULTRAVIOLET CURING OF RUBBERWOOD FIBRES –
UNSATURATED POLYESTER COMPOSITES**

by

KOSHEELA DEVI POO PALAM

**Thesis submitted in fulfilment of the
requirements for the degree
of Master of Science**

JANUARY 2005

ACKNOWLEDGEMENTS

I would like to express my greatest gratitude to my supervisor, Assoc. Prof. R.N. Kumar, for devoting his priceless time and sharing his knowledge and experiences and to my co-supervisors Prof. Rozman Hj. Din and Prof. Wan Rosli Wan Daud for their guidance, commitment and patience in making this research into a reality. I sincerely submit my most appreciation to Dr. Mazlan Ibrahim for his guidance in my project and Assoc. Prof. Rokiah Hashim for allowing me to use her lab equipments.

I would like to extend my sincere thanks to Mr. Abu and Mr. Azizan, who helped in setting up equipments for pulping process and testing of fibres without much delay; Mrs. Nor Aida, Tuan Haji Ishak and Mr. Mat for providing me chemicals and lab equipments; Mr. Maarof for helping me out in setting up Instron for mechanical testing of my samples; Miss Jamilah for operating SEM testing; Mr. Johari and Mr. Mano for their guidance in using Image Analyzer.

My endless appreciation and indebtedness goes to Tang Lee Han, Guan Seng, Faiza, Rosyanty, Elia, Fatimah, Zian and Puteri for their encouragements during the most critical time, in the hour of need and frustration. The assistance and moral support from other colleagues and friends is also appreciated. I also gratefully acknowledge Ministry of Science, Technology and Innovative for sponsoring my study.

Finally I would like to dedicate this thesis to my beloved parents, Poo Palam and Sim Yook Lean and my siblings for their prayers, encouragements and support. An extraordinary dedication is addressed to Ganesh. Your love, patience and support were the catalyst in completing this thesis.

TABLE OF CONTENTS

		Page
ACKNOWLEDGEMENT		ii
TABLE OF CONTENTS		iii
LIST OF TABLES		viii
LIST OF FIGURES		x
LIST OF PLATES		xv
LIST OF ABBREVIATION		xvi
LIST OF SYMBOLS		xviii
LIST OF APPENDICES		xix
ABSTRAK		xx
ABSTRACT		xxii
CHAPTER 1: INTRODUCTION		
1.1	Introduction	1
1.2	Research Objectives	8
CHAPTER 2: LITERATURE REVIEW		
2.1	Radiation Curing	9
	2.1.1 Ultraviolet Radiation	10
	2.1.1.1 Introduction	10
	2.1.1.2 Principles of Photoinitiation	14
	2.1.1.2.1 Population of the Chemical Reactive Excited State	14
	2.1.1.2.1.1 Light Absorption	14
	2.1.1.2.1.2 Intersystem crossing and the Nature of Excited States	16
	2.1.1.2.1.3 Photosensitization	18
	2.1.1.2.2 Initiator Radical Formation	19
	2.1.1.2.3 Initiation and Propagation	20
	2.1.1.2.4 Efficiency of Photoinitiation	21
	2.1.1.3 Selection of Photoinitiator	22

2.1.1.3.1	Biscaylphosphine oxides	23
2.1.1.3.2	1-Hydroxy-cyclohexyl-phenyl-ketone (HCPK)	26
2.2	Composite Materials	27
2.2.1	Classification of Composite Materials	27
2.2.2	Matrix Materials	29
2.2.2.1	Thermosetting Resins	30
2.2.2.1.1	Unsaturated Polyester Resin	31
2.2.2.2	Thermoplastic Resins	33
2.2.3	Fibre Reinforcement	34
2.2.4	Lignocellulosic as Reinforcement in Thermoset Composites	35
2.2.4.1	Source and Availability of Lignocellulose Fibres	36
2.2.4.2	Chemical Composition of Lignocellulose Fibres	38
2.2.4.2.1	Cellulose	39
2.2.4.2.2	Hemicelluloses	40
2.2.4.2.3	Lignin	41
2.2.4.2.4	Pectin and Waxes	41
2.2.4.3	Mechanical Properties of Lignocellulose Fibres	42
2.2.5	Fibre Matrix Interface	43
2.2.6	Rubberwood Fibre and Its Composites	44
2.3	Pulping for the Preparation of Bio-fibre Reinforcement	49
2.3.1	Introduction to Pulping	49
2.3.2	Types of Pulping Processes	50
2.3.2.1	Mechanical Pulping	50
2.3.2.2	Chemical Pulping	52
2.3.2.2.1	Kraft Process	52
2.3.2.2.1.1	Terms Used in Kraft Pulping	54
2.3.2.2.1.2	Process Conditions and Variables	55
2.3.2.2.1.3	Properties of Kraft Pulps	58
2.3.2.2.1.4	Additives in Kraft Pulping	59
2.3.2.2.2	Sulfite Process	62
2.3.2.3	Semi-chemical Pulping	63

CHAPTER 3: STATISTICAL EXPERIMENTAL DESIGN

3.1	Statistical Techniques in Experimentation	65
3.2	Response Surface Methodology (RSM)	67
3.2.1	Central Composite Design	69

CHAPTER 4: MATERIALS AND METHODOLOGY

4.1	Materials for Making Bio-fibre Composites	72
4.1.1	Matrix	72
4.1.1.1	Unsaturated Polyester Resin	72
4.1.1.2	Photoinitiator	72
4.1.2	Reinforcement Fibres	74
4.1.2.1	Rubberwood Fibres	74
4.1.3	Materials for AQ-Kraft Pulping process	75
4.1.3.1	Sodium Hydroxide (NaOH)	75
4.1.3.2	Sodium Sulfide (Na ₂ S)	75
4.1.3.3	Anthraquinone (C ₁₄ H ₈ O ₂)	75
4.2	Methodology	76
4.2.1	AQ-Kraft Pulping Process	77
4.2.2	Preparation of Composites	81
4.2.2.1	Preparation of Non-woven Reinforcing Bio-fibre Mat	81
4.2.2.2	Matrix Preparation	83
4.2.2.3	Impregnation of Fibre Mat	84
4.2.2.3.1	Impregnation of Bio-fibre Mat with 'Matrix Resin'	84
4.2.2.3.2	Impregnation of Bio-fibre Mat with Different Weight	84
4.2.2.4	UV Irradiation of the Impregnated Mat	85
4.3	Testing and Characterization	86
4.3.1	Mechanical Testing	86
4.3.1.1	Tensile Test (ASTM D 638)	86
4.3.1.2	Flexural Test (ASTM D 790)	86
4.3.1.3	Izod Impact Test (ASTM D 256)	88
4.3.1.4	Water Absorption of Composites (ASTM D 570)	88
4.3.1.5	Kappa number of pulp (TAPPI – T 236cm- 85)	89

4.3.1.6 Brightness of pulp (TAPPI – T 425 om-92)	91
4.3.1.7 Gel content	91
4.3.1.8 Image Analyzer	92
4.3.1.9 Scanning Electron Microscopy (SEM)	92
4.3.1.10 Dynamic Mechanical Thermal Analysis (DMTA)	92

CHAPTER 5: RESULTS AND DISCUSSION

5.1	Reaction Scheme of Cross-linking/Grafting of Unsaturated Polyester Resin on to Bio-fibre Induced by Photoinitiators (IRGACURE 1800)	95
5.2.	Effect of Pulping on Physical & Mechanical Properties of Bio-fiber Composites	103
5.3	Necessity to Delignify the TMP Fiber	105
5.4	Effect of Pulping Variables on Physical and Mechanical Properties of AQ-kraft Pulped Fibre Composites	111
5.4.1	Effect of Pulping Variables on Tensile Strength of AQ-kraft Pulped Fibre Composites	116
5.4.2	Effect of Pulping Variables on Flexural Strength of AQ-kraft Pulped Fibre Composites	143
5.4.3	Effect of Pulping Variables on Impact Strength of AQ-kraft Pulped Fibre Composites	149
5.4.4	Effect of Pulping Variables on Water Absorption at Equilibrium Level of AQ-kraft Pulped Fibre Composites	154
5.4.5	Effect of Pulping Variables on Thickness Swelling at Equilibrium Level of AQ-kraft Pulped Fibre Composites	155
5.4.6	Effect of Pulping Variables on Gel Content of AQ-kraft Pulped Fibre Composites	156
5.5	Optimization	158
5.6	Effect of Percentage of Fibre Content on Mechanical Properties of AQ-kraft Pulped Fibre Composites	161
5.7	Effect of Concentration of Photoinitiator on Mechanical Properties of AQ-kraft Pulped Fibre Composites	166
5.8	Influence of UV Lamp Doped with Gallium and Indium on Mechanical Properties of AQ-kraft Pulped Fibre Composites	172

5.9	Characterization of TMP Fibre Composites and AQ-kraft Pulped Fiber Composites	183
5.9.1	Scanning Electron Microscopy (SEM)	183
5.9.2	Dynamic Mechanical Thermal Analysis of TMP Fibre Composites and AQ-kraft Pulped Fibre Composites	196

CHAPTER 6: CONCLUSIONS

6.1	Conclusions	201
6.2	Suggestion for Future Research	207

BIBLIOGRAPHY		208
---------------------	--	-----

APPENDICES

Appendix A:	Relative spectral distribution of standard UV lamp.
Appendix B:	Relative spectral distribution of doped UV lamp.
Appendix C:	Statistical analysis on tensile strength of AQ-kraft pulped fibre composites.
Appendix D:	Statistical analysis on kappa number of AQ-kraft pulped fibers
Appendix E:	Statistical analysis on the fiber length of AQ-kraft pulped fibres
Appendix F:	Statistical analysis on the brightness of AQ-kraft pulped fibres
Appendix G:	Statistical analysis on flexural strength of AQ-kraft pulped fibre composites
Appendix H:	Statistical analysis on impact strength of AQ-kraft pulped fibre composites

LIST OF TABLES

	Page
Table 2.1: Chemical composition of some common lignocellulose fibres.	38
Table 2.2: Chemical composition of rubberwood.	46
Table 2.3: Definition of kraft pulping terms.	54
Table 4.1: Specification of Reversol P9728.	72
Table 4.2: The coded and real values of the factorial levels 4 factors in kraft pulping process.	80
Table 4.3: Real level CCD matrix for 4 factor in kraft pulping process.	80
Table 4.4: Weight of bio-fibres and unsaturated polyester.	84
Table 4.5: Factors f to correct for different percentage of permanganate used.	90
Table 5.1: Comparison of mechanical properties of TMP fibre composites and AQ-kraft pulped fibre composites.	106
Table 5.2: Effect of pulping variables on the properties of TMP-fibre & AQ-kraft pulped fibres	114
Table 5.3: The coded and real values of the 4 factorial levels in AQ-kraft pulping process.	114
Table 5.4: Effect of pulping variables on the properties of TMP fibre composite & AQ-kraft pulped fibre composite.	115
Table 5.5: Effect of pulping variables on water absorption, thickness swelling and gel content of TMP fibre composites & AQ-kraft fibre composites.	157
Table 5.6: Constraints applied for optimization	159
Table 5.7: Suitable combinations of optimization on AQ-kraft pulping process to acquire AQ-kraft composite with optimized physical and mechanical properties.	160
Table 5.8: Effect of weight percent of AQ-kraft pulped fibres on tensile strength, MPa of AQ-kraft pulped fibre composite.	162
Table 5.9: Analysis of Variance of the tensile strength MPa, data	162

Table 5.10:	Effect of weight percent of AQ-kraft pulped fibres on flexural strength, MPa of AQ-kraft pulped fibre composite.	163
Table 5.11:	Analysis of Variance of the flexural strength MPa, data	163
Table 5.12:	Effect of weight percent of AQ-kraft fibres on impact strength, kJ/m ² of AQ-kraft composite.	164
Table 5.13:	Analysis of Variance of the impact strength kJ/m ² , data	164
Table 5.14:	Effect of curing variables on the properties of AQ-kraft pulped fibre composites	177

LIST OF FIGURES

	Page
Figure 2.1: A typical energy level diagram.	17
Figure 2.2: Orbital interaction proposed to lead to conjugation between the carbonyl and the phosphoryl group.	25
Figure 2.3: Photolytic α -cleavage of Bis(2,6-dimethoxybenzoyl)-2,4,4-trimethyl-pentylphosphineoxide.	26
Figure 2.4: Photolytic α -cleavage of 1-Hydroxy-cyclohexyl-phenyl-ketone	26
Figure 2.5: Shows the chair conformation of glucose units and the β -1,4 linkage that cellulose polymer adopts in space.	39
Figure 2.6: Partial structure of O-acetyl-4-o-methylglucuronoxylan from hardwood	40
Figure 2.7: Partial structure from of type of lignin	41
Figure 3.1: Typical response surface plots encountered in chemistry i) a maximum response, ii) a minimum response and iii) a saddle point	68
Figure 4.1: 25 % Bis(2,6-dimethoxybenzoyl)-2,4,4-trimethyl-pentylphosphineoxide	73
Figure 4.2: 75 % 1-Hydroxy-cyclohexyl-phenyl-ketone (IRGACURE [®] 184)	73
Figure 4.3: Absorption spectrum of IRGACURE [®] 1800 (% in acetonitrile)	74
Figure 4.4: Chemical structure of anthraquinone	75
Figure 4.5: Process flow chart for making the composites from rubber wood fibres by ultra violet irradiation	76
Figure 4.6: Relations between various parameters used to express the results of a dynamic mechanical measurement	93
Figure 5.1: Photolytic α -cleavage of Bis(2,6-dimethoxybenzoyl)-2,4,4-trimethyl-pentylphosphineoxide	96
Figure 5.2: Photolytic α -cleavage of 1-Hydroxy-cyclohexyl-phenyl-ketone	98
Figure 5.3: Reaction scheme of initial stage in photocuring reaction	100

Figure 5.4:	Reaction scheme of possible polymerization and grafting reactions which occurs during the photocuring reaction.	101
Figure 5.5:	Tensile strength of AQ-kraft pulped fibres as a response of 4 factors in perturbation plots.	117
Figure 5.6:	3D response surface plot of tensile strength as a function of % active alkali, (x_1) and % sulfidity, (x_2) at cook in coded values.	118
Figure 5.7:	3D response surface plot of tensile strength as a function of temperature, (x_3) and time, (x_4) at cook in coded values.	119
Figure 5.8:	Kappa number of AQ-kraft pulped fibres as a response of 4 factors in perturbation plots.	123
Figure 5.9:	3D response surface plot of kappa number as a function of % active alkali, (x_1) and % sulfidity, (x_2) at cook in coded values.	124
Figure 5.10:	Cleavage of β -aryl ether bonds in non-phenolic phenylpropane units during pulping.	126
Figure 5.11:	Main reactions of the phenolic β -aryl ether structures during (alkali soda) and kraft pulping (Sjöström, 1981). R = H, alkyl or aryl group.	127
Figure 5.12:	3D response surface plot of kappa number as a function of temperature, (x_3) and time, (x_4) at cook in coded values.	129
Figure 5.13:	Fibre length of AQ-kraft pulped fibres as a response of 4 factors in perturbation plots.	133
Figure 5.14:	3D response surface plot of fibre length as a function of % active alkali, (x_1) and % sulfidity, (x_2) at cook in coded values.	134
Figure 5.15:	3D response surface plot of fibre length as a function of % temperature, (x_3) and time, (x_4) at cook in coded values.	135
Figure 5.16:	Brightness of AQ-kraft pulped fibres as a response of 4 factors in perturbation plot.	140
Figure 5.17:	3D response surface plot of brightness as a function of % active alkali (x_1), % sulfidity (x_2) at cook in coded values.	141
Figure 5.18:	3D response surface plot of brightness as a function of % sulfidity, (x_2) and time, (x_4) at cook in coded values.	142
Figure 5.19:	Flexural strength of AQ-kraft pulped fibre composites as a response of 4 factors in perturbation plot.	145
Figure 5.20:	3D response surface plot of flexural strength as a function of % active alkali (x_1), % sulfidity (x_2) at cook in coded values.	146

Figure 5.21:	3D response surface plot of flexural strength as a function of % temperature, (x_3) and time, (x_4) at cook in coded values.	147
Figure 5.22:	Impact strength of AQ-kraft pulped fibre composites as a response of 4 factors in perturbation plot.	150
Figure 5.23:	3D response surface plot of impact strength as a function of % active alkali (x_1), % sulfidity (x_2) at cook in coded values.	151
Figure 5.24:	3D response surface plot of impact strength as a function of % temperature, (x_3) and time, (x_4) at cook in coded values.	152
Figure 5.25:	Effect of fibre weight percent on the water absorption at equilibrium.	165
Figure 5.26:	Effect of % photoinitiator on tensile strength of AQ-kraft pulped fibre composites.	169
Figure 5.27:	Effect of % photoinitiator on flexural strength of AQ kraft fibre composites.	169
Figure 5.28:	Effect of % photoinitiator on impact strength of AQ-kraft fibre composite.	170
Figure 5.29:	Effect of % photoinitiator on % water absorption at equilibrium level.	171
Figure 5.30:	Effect of percentage of photoinitiator on tensile strength of AQ-kraft pulped fibre composites.	179
Figure 5.31:	Effect of percentage of photoinitiator on flexural strength of AQ-kraft pulped fibre composites.	180
Figure 5.32:	Effect of percentage of photoinitiator on impact strength of AQ-kraft fibre composites.	180
Figure 5.33:	Effect of percentage of photoinitiator on percentage of water absorption at equilibrium of AQ-kraft fibre composites.	182
Figure 5.34.a:	SEM micrograph of TMP fibre composites at magnification of 1.51X. The micrograph shows the surface of TMP fibre.	184
Figure 5.34.b:	SEM micrograph of TMP fibre composites at magnification of 3.99X. The micrograph shows the surface of TMP fibre and the adhesion of fibre.	184
Figure 5.34.c:	SEM micrographs of TMP fibre composites at magnification of 500 X. The micrograph shows fibre pull out from the matrix.	185

Figure 5.34.d: SEM micrograph of TMP fibre composites at magnification of 100X. The micrographs shows presence of air bubbles in the composites.	186
Figure 5.35.a: SEM micrograph of AQ-kraft pulped fibre composites at magnification of 4.01 X. The micrograph shows rough surface of fibre from kraft pulped fiber.	189
Figure 5.35.b: SEM micrograph of AQ-kraft pulped fibre composites at magnification of 1.50 X. The micrograph shows no fbre pull out observed.	189
Figure 5.35.c: SEM micrograph of AQ-kraft pulped fibre composites at magnification of 500 X. The micrograph shows good fibre matrix interaction.	190
Figure 5.36.a: SEM micrograph of AQ-kraft pulped fibre composites at magnification of 4.00X. The micrograph shows the surface of kraft pulped fibre.	191
Figure 5.36.b: SEM micrograph of AQ-kraft pulped fibre composites at magnification of 1.5 X. The micrograph shows no fbre pull out being observed and better adhesion.	191
Figure 5.36.c: SEM micrograph of AQ-kraft pulped fibre composites at magnification of 500X. The micrograph shows no fibre pull out being observed and better adhesion.	192
Figure 5.37.a: SEM micrograph of AQ-kraft pulped fibre composites at magnification of 4.04 X. The micrograph shows surface of the kraft pulped composites	193
Figure 5.37.b: SEM micrograph of AQ-kraft pulped fibre composites at magnification of 1.51 X. The micrograph shows no fbre pull out being observed and better adhesion.	193
Figure 5.37.c: SEM micrograph of AQ-kraft pulped fibre composites at magnification of 1.5 X. The micrograph shows no fbre pull out being observed and better adhesion.	194
Figure 5.38: Variation of storage modulus (E'), loss modulus (E'') and tan δ as a function of temperature for TMP fiber composites.	198
Figure 5.39: Variation of storage modulus (E'), loss modulus (E'') and tan δ as a function of temperature for AQ-kraft pulped fiber composites.	198

- Figure 8.1:** Relative spectral distribution of standard mercury UV lamp.
- Figure 8.2:** Relative spectral distribution of standard mercury doped with gallium and indium.
- Figure 8.3:** Normal probability plot for tensile strength.
- Figure 8.4:** Residual analysis for tensile strength.
- Figure 8.5:** Normal probability plot for kappa number.
- Figure 8.6:** Residual analysis for kappa number.
- Figure 8.7:** Normal probability plot for length of AQ-kraft fibres.
- Figure 8.8:** Residual analysis for length of AQ-kraft fibres.
- Figure 8.9:** Normal probability plot for brightness of AQ-kraft fibres.
- Figure 8.10:** Residual analysis for brightness of AQ-kraft fibres.
- Figure 8.11:** Normal probability plot for flexural strength of composites.
- Figure 8.12:** Residuals analysis for flexural strength of composites.
- Figure 8.13:** Normal probability plot for impact strength of composites
- Figure 8.14:** Residuals analysis for impact strength of composites

LIST OF PLATES

	Page
Plate 4.1: A stationary stainless steel digester, NAC Autoclave Co. Ltd., Japan	78
Plate 4.2: A mechanical disintegrater, Autotest HPP-100	79
Plate 4.3: Deckle box used for formation of bio-fibre mat	83
Plate 4.4: UV irradiator IST UV machine, Strahlentechnik metz gmbh, Model M20-1-Tr-SLC	85

LIST OF ABBREVIATIONS

E_T	Triplet energy
S_0	Ground state
S_1, S_2	Excited singlet state
T_1, T_2	Excited triplet state
$h\nu$	UV irradiation
SMC	Sheet Moulding Compound
UV	Ultra Violet
EB	Electron Beam
VOC	Volatile Organic Compound
TMP	Thermo-mechanical pulping
RSM	Responses Surface Methodology
CCD	Central composite design
O.D	Optical density
HCPK	1-Hydroxyl-cyclohexyl phenyl ketone
FRP	Fibre Reinforced Plastic
RMP	Refiner Mechanical Pulp
CTMP	Chemithermo Mechanical Pulp
AQ	Anthraquinone
AMS	Anthraquinone-2-monosulfate
MOR	Modulus of Rapture
MDF	Medium density fiber board
SEM	Scanning Electron Microscopy
DMTA	Dynamic Mechanical Thermal Analysis
LCC	Lignin-Carbohydrate Complexes

NaOH	sodium hydroxide and
Na ₂ S	sodium sulfide
H ₂ O ₂	hydrogen peroxide
Fe ²⁺	Ferrous ion
E'	storage modulus
E''	loss modulus
tan δ	the damping or internal friction
nm	nanometer

LIST OF SYMBOLS

T_g	glass transition temperature
ϵ	extinction coefficients
W_{pu}	Air dry weight of pulp, g
W_{st}	Oven dry weight of TMP rubberwood fiber, g
MC_p	Moisture content of pulp (based on air dry), %
σ_f	Stress in the outer fibre at midpoint, (MPa)
E_B	Modulus of elasticity in bending, Nm^{-2}
W_w	wet weight of sample, g
W_c	conditioned weight of sample, g
W_0	weight of sample before extraction, g
W_1	weight of sample after extraction, g

LIST OF APPENDICES

- Appendix A:** Relative spectral distribution of standard UV lamp.
- Appendix B:** Relative spectral distribution of doped UV lamp.
- Appendix C:** Statistical analysis of tensile strength on the AQ-kraft pulped fibre composites.
- Appendix D:** Statistical analysis on kappa number of AQ-kraft pulped fibers
- Appendix E:** Statistical analysis on the fiber length of AQ-kraft pulped fibres
- Appendix F:** Statistical analysis on the brightness of AQ-kraft pulped fibres
- Appendix G:** Statistical analysis on flexural strength of AQ-kraft pulped fibre composites
- Appendix H:** Statistical analysis on impact strength of AQ-kraft pulped fibre composites

PEMATANGAN KOMPOSIT GENTIAN KAYU GETAH – POLIESTER TAK TEPU MELALUI SINARAN ULTRA UNGU (UV)

ABSTRAK

Kajian ini telah dijalankan untuk mengkaji sifat-sifat fizikal dan mekanikal komposit gentian semulajadi yang mempunyai sifat nilai tambah yang dihasilkan melalui teknik pematangan mesra alam iaitu sinaran ultra-ungu (UV) (lampu UV merkuri piawai digunakan). Resin poliester tak tepu digunakan sebagai polimer matriks bersama dengan pemula foto bisasilfosfin oksida. Gentian kayu getah dari pemulpa termomekanikal (TMP) dipilih sebagai gentian penguat. Gentian ini merupakan bahan buangan dari salah satu syarikat penghasilan bod gentian ketumpatan sederhana (MDF). Kajian awal menunjukkan gentian TMP tidak dapat diimpregnasi dengan resin dengan baik, berkemungkinan disebabkan oleh sifat ketumpatan pukal yang rendah di samping dengan kehadiran lignin pada permukaan gentian. Untuk mengatasi masalah tersebut, pemulpaan kraft-antrakuinon (AQ-kraft) yang terkenal dengan kelebihan dari segi penyingkiran lignin secara berkesan dan penghasilan gentian yang kuat telah digunakan dalam kajian ini. Selain itu, proses ini juga dijangka dapat meningkatkan pelekatan antaramuka gentian-matriks. Pembolehkan dalam operasi pemulpaan dianggap mempunyai kesan ke atas sifat kekuatan gentian. Oleh itu, kaedah respon permukaan (Response Surface Methodology, RSM) telah digunakan untuk mengkaji faktor-faktor yang mempengaruhi pemulpaan seperti (i) aktif alkali (ii) sulfiditi (iii) suhu pemulpaan dan (iv) masa pemulpaan ke atas sifat mekanikal komposit, darjah pematangan komposit, penyerapan air dan kestabilan terma komposit. Fungsi matematik yang diperolehi dari analisis data di atas telah digunakan bagi menunjukkan secara grafik plot respon permukaan 3D dan plot "perturbation". Kondisi pemulpaan yang optimum untuk penghasilan komposit yang kuat telah dikaji iaitu melalui

penggunaan 17.0 % aktif alkali, 27.0 % sulfiditi, 162 °C suhu pemulpaan dan 95 minit masa pemulpaan. Kajian menyeluruh juga telah dijalankan terhadap faktor peratusan pemula foto (1.0-4.0 %), peratusan berat gentian (10-20 %) dan masa pendedahan sinaran ultra ungu (8-16 laluan) ke atas sifat komposit yang dihasilkan dari kondisi optimum. Didapati bahawa sifat mekanikal komposit dan ketahanan terhadap penyerapan air berasaskan gentian AQ-kraft adalah lebih baik berbanding komposit berasaskan gentian TMP. Komposit berasaskan gentian AQ-kraft juga didapati mempunyai kandungan gel yang lebih tinggi. Kajian mikroskop penskanan elektron (SEM) dijalankan ke atas komposit berasaskan kedua-dua jenis gentian untuk menyokong keputusan di atas. Analisis dinamik mekanikal terma (DMTA) menunjukkan nilai puncak $\tan \delta$ (115.09 °C) dan T_g (0.36 MPa) bagi komposit berasaskan gentian AQ-kraft adalah lebih rendah berbanding komposit berasaskan gentian TMP iaitu (124.39 °C dan 0.50 MPa). Ini berpunca dari penguncian mekanikal yang lebih baik di antara gentian dan matriks dan kesan dari cantuman poliester tak tepu pada gentian. Peningkatan peratusan gentian (10-20 %) dalam komposit didapati menurunkan kekuatan tensil, kekuatan fleksural, hentaman dan ketahanan terhadap penyerapan air. Sifat mekanikal komposit turut meningkat dengan peningkatan peratusan pemula foto sehingga mencapai tiga peratus. Selain lampu UV merkuri piawai, lampu UV disalut gallium dan indium turut digunakan dalam kajian ini. Komposit yang dimatangkan di bawah sinaran lampu UV disalut gallium dan indium memerlukan bilangan laluan sinaran UV (12 laluan) dan peratusan pemula foto yang lebih rendah (2.0 %) untuk memperolehi kandungan gel yang tinggi (98.44-99.46 %). Walau bagaimanapun, sifat mekanikal komposit ini didapati lebih rendah berbanding komposit termatang dengan lampu UV merkuri piawai. Oleh itu, didapati penggunaan lampu UV merkuri piawai dan foto pemula "peluntur foto" iaitu IRGACURE® 1800 adalah lebih sesuai untuk penghasilan komposit gentian semulajadi ini.

ULTRA VIOLET CURING OF RUBBERWOOD FIBRES - UNSATURATED POLYESTER COMPOSITES

ABSTRACT

This research project was carried out to study the physical and mechanical properties of value added bio-fibre composites made by employing environmentally benevolent ultra violet (UV) curing technique. Standard mercury UV lamp was used for the investigation. Unsaturated polyester resin along with bisacylphosphine oxide was used as polymer matrix. Rubberwood fibre (TMP fibres) residues, a waste and unutilized fibre from one of the medium density fibre board (MDF) plants, were used as reinforcement fibres. Un-delignified TMP fibre mats could not be impregnated due to its high bulk factor. Improper cure of the composites was also expected due to the presences of lignin in the fibres. To overcome this problem and to enhance the interfacial adhesion between the matrix and fibre, anthraquinone-kraft (AQ-kraft) pulping known for its efficiency in the removal of lignin and for producing high strength fibre was adopted. Since the operating variables of pulping process control the ultimate strength of the fibre reinforcement, Response Surface Methodology (RSM) was employed to investigate the effect of the following pulping parameters (i) active alkali (ii) sulfidity (iii) temperature and (iv) time of cooking on the responses such as mechanical properties of composites, degree of cure, water absorption and thermal stability. Mathematical functional relations obtained for the analysis of the above data were used both to represent graphically as 3D surface response plots and perturbation plots. Optimum pulping conditions for maximizing the strength of composites were established by employing optimization with constraints. The optimum conditions are 17.0 % active alkali, 27.0 % sulfidity, 162 °C pulping temperature and 95 minutes of pulping time. Effect of percentage of photoinitiators (1.0- 4.0 %), fibre content

(10-20 %) and the exposure time to UV (8-16 passes) on properties of these composites were studied under the above optimum condition. The mechanical properties of AQ-kraft pulped fibre composites showed properties superior to TMP fibre composites. Gel content and resistance towards water were better in AQ- kraft pulped fibre composites. Scanning electron microscopy (SEM) studies were carried out on both the type of fibre composites to confirm above findings. Dynamic mechanical thermal analysis (DMTA) showed the peak of $\tan \delta$ (0.36 MPa) and T_g (115.09 °C) for AQ-kraft pulped fibre composites was lower than TMP fibre composites 0.50 MPa and 124.39 °C respectively. This was due to better mechanical interlocking between the fibres and the grafted unsaturated polyester in AQ-kraft pulped fibre composites. Increase in weight percentage of fibres (10-20 %) in the composites decreased the tensile strength, flexural strength, impact strength and resistance towards water. The mechanical properties increased with increase of photoinitiator percentage up to 3 % and then decreased. Besides normal UV lamp, UV lamp doped with gallium and indium was also employed. Composites cured with doped lamp required lesser exposure time (12 passes) and lower percentage of photoinitiators (2 %) to affect same degree of cure (98.44-99.46 %). However, the mechanical properties of the composites were found to be lower than those produced from standard UV lamp. AQ-kraft pulped fibre composites can thus be made by using standard UV lamp instead doped lamp and photobleaching photoinitiator, IRGACURE® 1800.

CHAPTER 1 INTRODUCTION

1.1 Introduction

In the past few decades, research and engineering interest has been shifting from monolithic materials to fibre reinforced polymer materials. The desire for increasingly lighter, stronger and stiffer materials has been the driving force behind the expansion and increasing usage of fibre reinforced polymer composites (Mohanty *et al.*, 2000). Fibre reinforced composites can be divided into two broad categories as have been identified as following; (1) price driven composites for which cost dictates the market; and (2) performance driven composites for which properties dictates the market (Teoh, 1998).

Price driven composites are composites made from bio-fibres as these fibres are cheaper than the synthetic fibres. Performance driven composites were the first composites which were made. Performance driven composites materials are composites made from, notably aramid, carbon and glass fiber reinforced plastics. These composites now dominate the aerospace, leisure, automotive, construction and sporting industries. Glass fibres are most widely used to reinforce plastic due to their low cost compared to aramid and carbon fibres and its fairly good mechanical properties. However, these fibres have serious drawbacks when compared to natural fibres (Wambua *et al.*, 2003).

Furthermore, for general purpose applications, where such high level of performance is superfluous, thus natural fibres can partly or completely substitute high performance fibres leading to price driven end uses. With this as primary objective

considerable research and development efforts are expended. In general, bio-fibre composites are mainly price driven commodity composites which will have just adequate properties for desired performance at relatively low cost (Teoh, 1998). Considerable amount of work has been done for making composites for high performance application by using natural fibres.

Moreover, the corresponding expansion in synthetic polymer production has led to increasing problems of recycling and resource identification (Peterson *et al.*, 2002). Governmental regulations and a growing environmental awareness throughout the world have triggered a paradigm shift towards designing materials compatible with the environment. Moreover, use of bio-fibres derived from annually renewable resources, as reinforcing fibres in both thermoplastic and thermoset matrix composites provide positive environmental benefits with respect to ultimate disposability and raw material renewability (Narayan, 1992). Therefore, attempts have been made to use natural fibre composites in place of glass fibre, mostly in non-structural applications. So far a good number of automotive components previously made with glass fibre composites are now being manufactured using environmentally friendly composites (Wambua *et al.*, 2003).

The Asian markets have been using natural fibres for many years. For example, jute is a common reinforcement in India. Natural fibres are increasingly being used in automotive in Europe. In 1999, consumption was 21,300 tons and by 2000 this had risen to 28,300 tons. Packaging is a further application in Europe, particularly in Germany. In North America wood/polymer composites amount to a 300,000 ton/year market for use in building and garden products, particularly decking (Bledzki *et al.*,

2002). Till date, the most important natural fibres are jute, flax, hemp and coir (Bledzki & Gassan., 1999).

Cellulosic fibres like henequen, sisal, coconut fiber (coir), jute, palm, bamboo, wood and paper in their natural condition as well as several waste cellulosic products such as shell flour, wood flour and pulp have been used as reinforcing components with different thermosetting and thermoplastic resins. These natural fibres could be profitably used in the manufacture of fibre polymer reinforced composites which possess attractive physical and mechanical properties (Bledzki *et al.*, 1999; Franco & Gonzalez, 2003). They impart as a result of desirable fibre aspect ratio, high stiffness and strength to the composites, biodegradability, readily available from natural sources and more importantly they have a low cost per unit volume basis (Bledzki *et al.*, 1999).

Besides the above advantages, natural fibre composites impart the process by reduced tool wear, reduced dermal and respiratory irritation, and high degree of flexibility (Karnani *et al.*, 1997). The latter is especially true since these fibres, unlike glass fibres will bend rather than fracture during processing. Whole natural fibres undergo some breakage while extensively mixed with the polymer matrix, but this is not as notorious as with brittle or mineral fibres (Franco & Gonzalez, 2003). Further, these products are completely degradable at the end of their use life, by means of biodegradation and/or combustion (Marcovich, 2001)

Natural fibres, however, hold some undesirable characteristics, which impede their successful utilization in composites. The undesirable characteristics include: 1) hydrophilic nature of the materials that results in poor interfacial adhesion and poor fiber dispersion in composites (Kazayawoko & Balatinecz, 1997); 2) hygroscopic

nature of the materials that leads to dimensional instability and poor composite performance when continuously exposed to high humidity environments (Sanadi *et al.*, 1997); and 3) poor thermal stability at the typical processing temperatures for thermoplastics (Kazayawoko & Balatinecz, 1997). These problems are usually reduced by appropriate surface modification which can produce important effects on dispersibility of fibres in the resin matrix and promotes better adhesion between polymer and filler (Marcovich, 2001).

These properties may be improved by physical treatments (cold plasma treatment, corona treatment) and chemical treatment (maleic anhydride, organosilanes, isocyanates, sodium hydroxide, permanganate and peroxide). Tripathy *et al.* (1999) found that delignification by bleaching produces better interfacial bond between jute fibre and polyester matrix and hence better mechanical properties of composites. Gassan *et al.* (1999) improved tensile, flexural strength and stiffness of jute-epoxy composites by treating the fibres with silane. Dynamic mechanical thermal analysis carried out on the polyester matrix composites showed that alkalized fibre composites with better compatibility between fibre and matrix have higher E' value and lower T_g values (Aziz & Ansell, 2004). Mansur *et al.* (1997), reported treatment of woody plant or use of chemithermo mechanical pulp (CTMP) of palm leaves resulted in composites with low void contents and high bending strength.

Recently, several researchers (Liew, 1998; Ismail *et al.*, 2001) showed some interest in using rubberwood fibres as reinforcement in thermoplastic and thermoset composites. Rubberwood (a standard name for the timber of *Hevea Brasiliensis*) is natural polymer that has gained special importance because of it is cheap and plentiful (Abu-Ilaiwi *et al.*, 2003). Ismail *et al.* (2001) have used rubberwood fibres, as filler in

natural rubber compounds and reported that the tensile modulus of the composites increases with the filler loading and incorporation of the filler reduces the elasticity of the rubber chain resulting in more rigid composites. Liew (1998) has carried out studies to evaluate the suitability of producing fibre-polypropylene composites using oil palm frond fibre and rubberwood fibres. Graft copolymerization of methyl methacrylate into rubber wood fiber using H_2O_2 and Fe^{2+} as an initiator system was carried by Ibrahim *et al.* (2003).

Many considerations are taken in selecting the proper matrix let it be thermoplastic or thermoset in the formation of composites. Thermoplastic biofibre composites have the limitation to be able to produce smaller moldings. For producing sheet and panel materials of large area, the thermoplastic composites are not suitable due to the operational constraints since such materials are not amenable to moulding process such as molding (injection molding, transfer molding, etc) normally employed for moulding thermoplastic. Thermosetting biofibre composites can, on the other hand, be produced in large sheets due to the processing techniques such as compression molding employing large hydraulic press both batchwise as well as continuous process. In principle the processing techniques of natural fibre composites can be similar to those of glass fibers. However, techniques in which continuous fibres are used (like pultrusion) or where fibres are chopped like spray-up or sheet moulding compounds (SMC), require some adjustment in fibre handling.

Although thermoplastics have the added advantage of recycling possibilities, thermosets are targeted to obtain much improved mechanical properties compared to thermoplastics in the resulting bio-composites (Mishara *et al.*, 2003). Normally, thermosetting resins like polyester, epoxy and phenolic are used as the polymeric

binding matrix. Unsaturated polyester resins (although slightly inferior to epoxy resins in overall properties) are chosen first for making fiber reinforced composites by any molder because of the ease of handling and fabrication and the low cost compared to other resins.

About 85% of the fiber reinforced composites products are manufactured using polyester resins (Saroja *et al.*, 1998). Unsaturated polyester resins have good balance of mechanical, electrical and chemical properties (Mishara *et al.*, 2003). Application of unsaturated polyester as polymer matrix in composites and cellulosic fibres as reinforcement has been widely reported (Albuquerque *et al.*, 1999; Devi *et al.*, 1997; Mwaikambo *et al.*, 1999; Marcovich, 2001). Although, composites based on unsaturated polyester matrices are well known, there are limited studies on the use of rubber wood fibre as reinforcing components along with this resin.

Most matrices used for high performance fiber reinforced composites are thermally cured thermoset resins (Thierry *et al.*, 2000). The systems used are either reacting step-wise, such as epoxy-amine systems, or chain-wise, such as styrene-unsaturated polyester. In a thermally initiated free radical polymerization, the initiator decompose when heated, producing radicals from which the reaction propagates. The reaction exotherm adds to the thermal energy supplied by the oven, leading to high temperatures in the core of the structure. Therefore, the cure of large and thick composites requires complex temperature programs to dissipate the heat of the reaction. This is to avoid too high temperatures in the composite which can result in blister, thermal degradation, internal stresses, etc. The process uses much energy since the composite must be slowly heated up to cure temperature and kept there for a long time. These problems can however be overcome by cure of radiation processing.

Radiation curing of composites is gaining significance for the promises it holds, and hence a good amount of work has been done and published in this field (Adanur & Arumugham, 2002). Electron beam curing, gamma radiation and lasers have been the radiation source in curing sources in majority of the work (Thierry *et al.*, 2000). Ultra violet (UV) radiation, a popular source in curing industry has not been extensively researched for the composites industry. However, UV curing of glass fibre reinforced composites has been investigated since the development of photo-bleaching initiators (Thierry *et al.*, 2000). The word photofabrication has been coined by CIBA-GEIGY to describe the process of making glass-fibre reinforced composite by exposure to UV radiation. This source of radiation offers several unique advantages for specific applications and has been researched in this work.

The main advantages of using UV radiation to initiate the chain reaction lies in the high polymerization rate that can be reached under intense illumination to ensure the liquid to solid phase change takes place within a short time (Tanihata, 1991). Efficient curing and consistent through cure occur by employing appropriate choice of UV lamp and photo-initiator combinations (Thierry *et al.*, 2000). The UV curing processes eliminates the use of peroxide employed in the conventional curing systems, which releases volatile organic compound (VOC) to environment and causes air pollution.

The UV process employs single pack resin system (resin containing photo-initiators), which have very long shelf life and the viscosity of the resin does not change during the impregnation process. This ensures consistency in the quality of the product, a feature non-existent in the currently used process using peroxide curing agents. Since the curing reaction goes near to completion, the residual styrene

emission is absent (VOC is absent), a desirable characteristic not achievable in peroxide based curing systems. In this respect it is unsurpassed by any other competitive process currently being employed for making similar products (Thierry *et al.*, 2000).

1.2 Research Objectives

In this study, an attempt was made to produce thermoset (unsaturated polyester) polymer matrix bio-fibre composites by using classifier rubberwood fibre residues available from a factory employing thermo-mechanical pulping (TMP) process. Fibers produced by TMP is too bulky, (entraps air between the fibres) to be efficiently impregnated with the matrix resin and the lignin content is high. Lignin being a good UV absorber can compete with the photoinitiator and substantially reduce the efficiencies of photocuring. On subjecting the TMP fibres to kraft pulping method, the bulk factor can be reduced along with effecting removal of lignin. Photo-fabrication technique was employed for the curing of the composites. Studies were performed to:

- i) Determine to effect of pulping variables on the properties of the composites.
- ii) Determine the optimum combinations of pulping parameters to obtain acceptable properties of pulp suitable for UV fabrication.
- iii) Determine the effect of the photofabrication variables such as percentage of photo-initiator, number of passes under UV irradiation, application of UV lamp with different wave lengths and fiber to resin ratio on the properties of composites.

In this study, RSM (Responses Surface Methodology) was employed in order to collect experimental data most efficiently within a short duration.

CHAPTER 2

LITERATURE REVIEW

2.1 Radiation Curing

Curing coatings by means of radiation represents one of the new techniques that are replacing the use of conventional or low solids, solvent borne coatings (Koleske, 2001). Radiation curable coatings refer to transformation of liquid formulations to solids which cover a surface of substrates by UV photons or electrons. During the sixties, the threat of energy shortages and environmental consciousness created a favorable climate for the development of radiation curing technology. It soon became apparent that the radiation curing technology was the only one answering the challenge of the future and modern finishing. It meets the 3 "E" rules fixed as a basic for each new development in the much diversified areas of coatings. The 3 "E" are Economy, Energy and Ecology (Tanihata, 1991).

Radiation curing technologies provide a number of economic advantages over the usual thermal operation among them; rapid through cure, low energy requirements, room temperature treatment, non polluting and solvent free formulations and low costs. The main sources of actinic energy for curing coatings by radiation are electron beam and ultraviolet light. In 1984, Pincus indicated that there were four suppliers of electron beam (EB) equipments and more than 40 suppliers of ultraviolet light (UV) equipment. Light beams are used to start photochemical and chemical reactions in organic materials (monomers, oligomers, polymers), to form a new polymeric material (Decker and Moussa, 1993).

The UV light and EB curing coatings and varnishes on various substrates of paints, adhesives, composites, etc. and the imaging area (UV curable inks, printing plates, high resolution relief imaging for microcircuits in electronics) represent a large class of industrial applications. Among various factors which affect the efficiency of the polymerization reaction, the photoinitiator has been recognized as key factor that governs, e.g. in coating applications, to some extent, curing speed, through cure, tack-free index and hardness (Fouassier *et al*, 2003).

In the past few years, most of the research efforts in the formulating UV-curable resins have been directed towards the development of more efficient photoinitiators and highly reactive nonirritating monomers, with the objective of increasing both the cure speed and the extent of the polymerization, as well as improving the final properties of the cured materials (Tanitaha, 1991). In coating applications, it is important to reduce as much as possible the amount of unreacted monomer, which is known to affect adversely the long term properties of UV cured polymers (Decker and Moussa, 1993).

2.1.1 Ultraviolet Radiation

2.1.1.1 Introduction

In general, ultraviolet light units operate with electromagnetic radiation that is in the optical region of 200-760 nm. They also produce infrared radiation of 760 nm to 1.0 mm, but this energy is thermal and acts as either to anneal the cured coating and relieve internal stress and strains or enhance cure rate in cationic cure systems. Of course, in certain formulations this thermal energy can have a deleterious effect by causing volatilization of reactants, and it is minimized in some equipment. In the other

cases, such as cationic UV curing, the thermal energy can be highly beneficial by kinetically enhancing the cure rate of the compounds.

Basically, in the case of UV curing, compounds susceptible to rapid polymerization are contacted with initiating species obtained by photolysis of a photoinitiator. In the UV cure such compounds, a photoinitiator that is capable of photolyzing or dissociating to active species is added to the formulation. When the light of proper wavelength strikes the photoinitiator, the active species are generated and polymerization takes place rapidly (Tanihata, 1991). Certain photoinitiators generate free radicals, and these are used to cure oligomers such as acrylates. Other photoinitiators generate cations, which are used to cure epoxide-based systems. It should be readily apparent that matching the out put of the photoinitiator is an important aspect of this technology.

There are a few different types' ultraviolet light technologies. These are medium pressure mercury vapor lamps, electrodeless vapor lamps, pulsed xenon lamps, metal halide and lasers. Medium pressure mercury vapor lamps have been used commercially for about 20 years (Tanihata, 1991). It produces approximately 29% UV over wide spectral range (200-400 nm) and is the most efficient of the available, high output lamps in converting electrical power to UV energy. The bulb is an evacuated quartz tube that contains metallic mercury and has electrodes at each end. When electrical energy is supplied through the electrodes and an arc is struck between them. This heats mercury in the tube to plasma state, which emits UV, visible and infrared radiation. The excitation spectral distribution of standard mercury UV lamp which is used in this study is given in the Appendix A. The systems can be doped to alter the emission spectrum, but usually only mercury is used (Dietliker, 1991).

Electrode lamps have been in use for about a decade and currently are very popular in the industry (Koleske, 2001). The vacuum in the tube (UV bulb) is manufactured from quartz, which is transparent to the UV radiation. The bulb contains either mercury or the other proprietary metals and gases. The system is activated by microwave or radiofrequency energy. Because of the nature of this activation system, it essentially has instant on and off operation.

Xenon lamps are quartz tube filled with doped xenon. The lamp is powered by pulsed electrical current. These units offer very low heat output along with short time, extremely high peak intensity output. The output spectrum is continuous with this source rather than that of the discrete line types as from the medium pressure mercury vapor lamps (Koleske, 2001). However in certain instances mercury is added to the tube contents to enhance curing in the region of mercury's spectral lines. The output has also been modified with other metals such as iron and beryllium.

Metal halide lamps are not a specific lamp type, but a variation on standard lamp obtained by introducing into the lamp, volatile metal halides, in addition to mercury and argon gas. These lamps are sometimes called "doped" or "additive lamps". The effect of these additives is to shift the spectral output towards the long wavelength end of the spectrum. Metal halides available are iodides of lead, iron, magnesium, gallium, indium, thallium and others and they can be used individually or in combination with each other (Dietliker, 1991). UV lamp doped with gallium and indium is used in this study to investigate the influence of UV lamp with different wavelength on the curing profile and mechanical properties of the composites. The excitation spectral distribution of doped UV lamp is given in Appendix B.

Metal halide lamps do offer potential advantages in some specific areas of application where the increased long wavelength radiations give better penetration (Dietliker, 1991). Some examples of use are:

- a) Gallium indium doped lamp for thick pigmented coatings
- b) White coatings using iron iodide lamp
- c) Screen printing on plastic by using gallium oxide or iron iodide lamps.

The limitation, so far in the use of metal halide lamps are:

- a) No universally applicable improvement in spectral output has been achieved
- b) Lamps are expensive and tend to have a shorter effective life
- c) Manufacture is limited to short lamps and lower power lamps and even these are not readily available
- d) It would be necessary to use these lamps in conjunction with standard lamps to achieve both, good surface and through cure in many instances.

Argon ion and nitrogen lasers in combination with specific photoinitiator that have a strong absorbance at the emission line of the laser have been used to cure multifunctional acrylates. Although the studies are interesting and may hold promise for the future, at present this is considered to be a research area of potential interest for the electronics industry (Tanihata, 1991).

2.1.1.2 Principles of Photoinitiation

Photoinitiation of radical polymerization involves three stages: (1) population of the chemically reactive excited state, which requires light absorption and may also involve intersystem crossing and photosensitization (2) formation of initiator radicals by photocleavages of the reactive excited state or by H-abstraction from H-donor and (3) initiation of polymerization by interaction of initiator radicals with reactive monomers and oligomers. These stages will be discussed in the section in general with particular emphasis on the factors that determine the efficiency of the photoinitiation (Tanihata, 1991).

2.1.1.2.1 Population of the Chemical Reactive Excited State

2.1.1.2.1.1 Light Absorption

The first step in photoinitiated polymerization is absorption of light energy by the photoinitiator. This requires that absorption bands of the photoinitiator overlap with the emission bands of the light source. An absorption spectrum of the photoinitiator may be obtained with an ultraviolet visible spectrophotometer. The resulting absorbance (A) or optical density (O.D) at each wavelength is convertible into molar absorptivities or extinction coefficients (ϵ) from the relationship:

$$\text{O.D} = \epsilon \cdot d \cdot c \quad (2.1)$$

where, d is the path length of the cell in cm, and c is the concentration of the initiator in M. The resulting ϵ values represent a measure of the probability of light absorption at each wavelength (Dietliker, 1991).

The above ϵ values signify that the light at 350 nm is absorbed relatively inefficiently. However two additional factors must be taken into account in UV curing. First one must consider emission spectrum of the light source. The ϵ value provides a measure of the proportion of the incident light (from the light source) which is absorbed. Thus if the intensity of the incident lamp is greater at 350 nm than at 250 nm, the number of photons absorbed at 350 nm relative to 250 nm is more than would be predicted from the corresponding ϵ values. It is the number of photons absorbed that determines the number of excited state photoinitiators produced (Dietliker, 1991). The second consideration is made apparent by a rearrangement of the above equation as follows:

$$d = O.D / \epsilon \cdot c \quad (2.2)$$

where d may be thought of as the depth of light penetration.

In this sense it is seen that the greater the ϵ value, the less penetration of the light at that wavelength. With reference to the aryl ketone photoinitiators at the concentrations utilized in UV curable coating and printing inks (1-10 %), most of the 250 nm light is absorbed at or near the surface, whereas the 350 nm light is available throughout the film. For most pigmented coating it is desired that the photoinitiator exhibit absorptivity in the near UV region in order to compete effectively with the pigment for the light energy. The presence of electron donating groups on the phenyl rings of aryl ketones generally results in higher absorptivity in this region. Absorptivity in the near UV visible light is also enhanced by the presence of an acylphosphine oxide and α -dicarbonyl groups (Dietliker, 1991).

2.1.1.2.1.2 Intersystem crossing and the Nature of Excited States

Most molecules in their ground state possess an even number of electrons which are spin paired and the electrons remain spin-paired in the excited states directly populated by light absorption. However, following the light absorption, spin unpairing may occur with facility, particularly in the case of aromatic ketones. The number of unpaired electrons in a particular state is known as spin multiplicity; and the terms singlet, doublet and triplet refer to no spin-unpaired electrons, one and two spin-unpaired electrons respectively.

Thus the light absorption by ground state singlets produces excited state singlet which may undergo spin-unpairing to yield excited state triplet. Such transformations between states of different spin-multiplicity are known as intersystem crossing. A typical energy level diagram is presented in Figure 2.1. The terms n, π^* and π, π^* refer to the orbital nature of the excited states (Dietliker, 1991).

Photochemical reactions are known to occur from both singlet and triplet excited states, and generally occur from the lowest excited singlet (S_1) and triplet (T_1) states. However due to the shorter lifetime of S_1 states (generally less than 10^{-8} seconds), many photochemical reactions particularly intermolecular processes occur via the T_1 states which are longer lived (generally greater than 10^{-6} seconds) (Dietliker, 1991).

Consequently, population of the chemically reactive state in the photoinitiator may require intersystem crossing, a factor which should be taken into account with regard to the overall efficiency of photoinitiation. Second important consideration is the

orbital nature of the excited states. For photoinitiator systems, the transitions of most interest are n,π^* and π,π^* which signify that an electron has been promoted from non-bonding (n) or bonding (π) orbital, respectively to an anti bonding (π^*) orbital. Of particular importance is the orbital nature of the reactive excited state which is generally the T_1 states. Generally, n,π^* states are more reactive in free radical reactions including both H-abstraction and photocleavage (Dietliker, 1991).

Absorption of light energy by a photoinitiator (PI) to produce an excited singlet state (eq.2.3), followed by intersystem crossing to the triplet state (eq.2.4) in competition with singlet decay, including both fluorescence and radiationless decay to the ground state (eq.2.5), are depicted below.

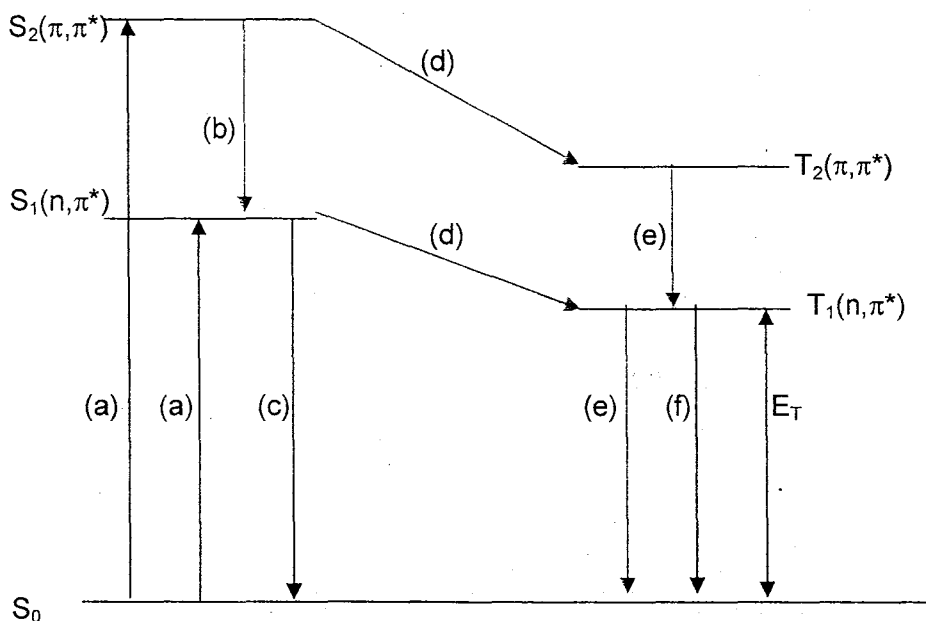
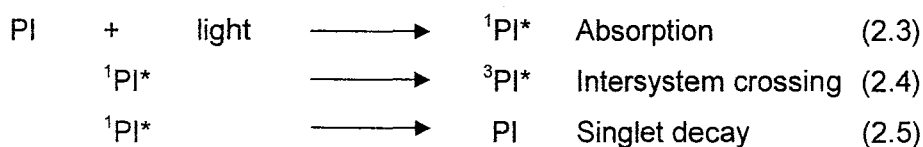
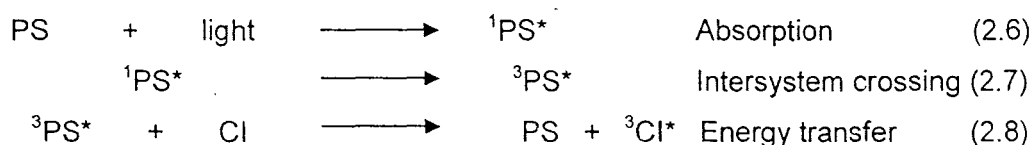


Figure 2.1: A typical energy level diagram

S_0	Ground state	(b)	Singlet decay (radiationless)
S_1, S_2	Excited singlet state	(c)	Singlet decay (fluorescence)
T_1, T_2	Excited triplet state	(d)	Intersystem crossing
\longrightarrow	Radiative process	(e)	Triplet decay
\longrightarrow	Radiationless process	(f)	Triplet decay
(a)	Light absorption	E_T	Triplet energy

2.1.1.2.1.3 Photosensitization

An alternative process populating the chemically-reactive excited state in photoinitiation is photosensitization. In this case, the photosensitizer (PS) absorbs the light energy (eq. 2.6), followed by intersystem crossing to the triplet state (eq. 2.7) and triplet-triplet energy transfer (eq.2.8) to produce the chemically-reactive state of the co-initiator (CI), which may undergo H-abstraction or photocleavage to produce initiator radicals.



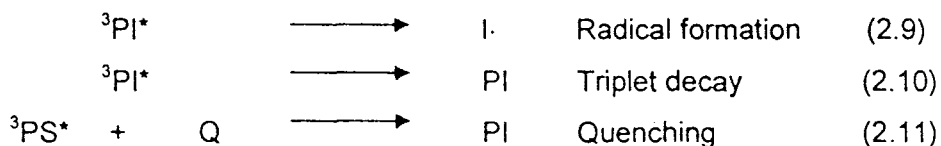
In photosensitization, the photosensitizer should possess desirable absorption characteristics as well as a high efficiency of intersystem crossing. Furthermore, efficient energy transfer requires that the triplet energy of the donor (PS) be greater than that of the acceptor (CI). That is the energy available from ${}^3\text{PS}^*$ should be greater than that required to produce ${}^3\text{CI}^*$ (Dietliker, 1991).

2.1.1.2.2 Initiator Radical Formation

Initiator radicals are produced from the reactive excited state by intramolecular photocleavage or intermolecular H-abstraction from a H-donor. An obvious advantage of photocleavage over H-abstraction mechanism is necessity of a bimolecular reaction in the latter case. That is, the generation of initiator radicals by H-abstraction requires that the photoinitiator interact with a H-donor, a process which may be limited by diffusion and with which other unproductive bimolecular reactions may compete (Dietliker, 1991).

On the other hand, the generation of initiator radicals by photocleavage requires that the reactive excited state must possess sufficient energy to allow efficient bond dissociation. In the case of reactive singlet state, radical formation competes with intersystem crossing to the triplet manifold and singlet decay to the ground state. More often, radical formation occurs via the lowest energy triplet state (T_1) as a consequence of its longer life-time. In this case, initiator radical formation (eq. 2.9) competes with triplet decay to the ground state (eq. 2.10) and various bimolecular quenching processes (eq. 2.11), including quenching by O_2 ($Q = O_2$), self-quenching ($Q = PI$), which is particularly important in the case of π, π^* triplets and quenching by monomer ($Q = M$) (Dietliker, 1991).

In this regard, it is pertinent that the longer lifetime of triplet state also make them more susceptible than singlet states to bimolecular quenching processes. Of course, it is mandatory that radical formation competes effectively with these quenching processes and particularly with quenching by oxygen when UV curing is carried out in air.



Photoinitiators that undergo this α -cleavage are benzoin derivatives, benzilketals, α -dialkoxyacetophenones, α -hydroxyalkylphenones, α -minoalkylphenones, acylphosphine oxides and methylbenzoin and 4-benzoyl-1,3-dioxolane derivatives. The majority of Type I photoinitiators are aromatic carbonyl compounds containing suitable substituents which facilitate direct photofragmentation, thereby producing radicals. An important criterion for Type I photoinitiator is the presence of a bond with a dissociation energy lower than the excitation energy of the reactive excited state but sufficiently high to provide adequate thermal stability (Tanihata, 1991).

Whereas photoinitiator that are under bimolecular photoinitiators are benzophenone/amines, Michler's ketone/benzophenone, thioxanthone/amines and miscellaneous aromatic ketones. The two main reaction pathways available for Type II photoinitiators are hydrogen abstraction by the excited initiator and photoinduced electron transfer, followed by fragmentation. Bimolecular hydrogen abstraction is typical reaction of diaryl ketones and is limited to this chemical type photoinitiators (Dietliker, 1991). Photoinduced electron transfer is more general process which is not limited to certain class of compounds and is more important as an initiation reaction.

2.1.1.2.3 Initiation and Propagation

Photoinitiated polymerization requires that the initiation process (eq. 2.12) competes effectively with recombination of initiator radicals (eq. 2.13), and reaction of initiator radicals with O_2 (eq. 2.14). Furthermore chain propagation (eq. 2.15) must

compete with O₂ addition (eq 2.16) and termination by initiator radicals (eq. 2.17) in order to produce appropriate chain lengths for desirable polymer characteristics.



2.1.1.2.4 Efficiency of Photoinitiation

The overall efficiency of photoinitiation is the product of the efficiencies at each stage of the process, including absorption, intersystem crossing (if required), initiator radical formation and initiation. Thus, the overall efficiency is the product of (1) fraction of incident light which is absorbed by the photoinitiator or photosensitizer, (2) the fraction of excited state singlet which is transformed into triplets, (3) the fraction of the triplets which yield initiator radicals and (4) fraction of radicals which initiates polymerization (Tanihata, 1991).

As indicated in the previous sections, the major competing processes are (1) singlet and triplet decay, (2) triplet quenching by O₂, monomer and ground state photoinitiator and (3) initiator radical recombination as well as reaction of initiator radicals with O₂. The reactions of initiator radical and O₂ with growing polymer chains also adversely affect the polymer properties in UV curing (Tanihata, 1991).

Generally, there is an optimal concentration of photoinitiator which is governed by efficient light utilization and initiator radical formation on the one hand opposed to self-quenching and light screening by the photoinitiator on the other (Tanihata, 1991). Light screening by the photoinitiator prevents through cure which adversely affects curing and may result in surface wrinkling, particularly with pigmented coatings.

2.1.1.3 Selection of Photoinitiator

The selection of a photoinitiator is the major concern in the development of a formulation. The photoinitiator has long been considered to determine only three properties of photocurable formulations, namely, cure speed, yellowing and cost. Whilst the photoinitiator does not influence these properties to large extent; it also plays an important role in determining other properties of the coating (Dietliker, 1991).

High photoinitiator efficiency is not only measured by cure rate, but also by through cure obtained under the curing conditions. The specific application in which the photopolymerizable formulation to be used dictates the relative importance of the criteria in the selection procedure. Equally important is the determination of the optimal condition for its use. The best photoinitiator can produce inadequate results if used under less optimal conditions (Dietliker, 1991).

Radical photopolymerization is highly complex process which includes many photochemical primary processes, subsequent and competing reactions. The rate at which the liquid system is solidified depends not only on the photochemical reaction, but also on the type of binder system, the initiating efficiency of the primary radicals and on external conditions such as the type and power of the irradiation source and the exposure time. The determination of optimum concentration of photoinitiator is also

crucial in order to obtain good results (Dietliker, 1991). Only by evaluating the optimum balance of the entire important parameters can the best curing properties can be obtained.

Literature study reveals among the radical type photoinitiators currently used in UV-curable systems, acylphosphine oxides have been found to give superior overall performance (Decker *et al.*, 2001). Recently, mixtures of acylphosphine oxides and α -hydroxyalkylphenone were introduced in the market providing advantages in white lacquer applications (Dietliker, 1991). Therefore, IRGACURE[®] 1800 a unimolecular photoinitiator which undergoes α -cleavage photofragmentation (Type I) was employed for the photofabrication of the bio-fibre composites.

IRGACURE[®] 1800 used is a mixture of 25 % Bis(2,6-dimethoxybenzoyl)-2,4,4-trimethyl-pentylphosphineoxide and 75 % 1-Hydroxy-cyclohexyl-phenyl-ketone. It exhibits outstanding curing performance in pigmented coating and affords minimum yellowing after exposure to sufficient amounts of UV radiation. Additionally the outstanding absorption properties of IRGACURE[®] 1800 allow curing of thick sections. IRGACURE[®] 1800 is thermally stable compounds and do not decompose below 180 °C

2.1.1.3.1 Biscaylphosphine oxides

Biscaylphosphine oxides have a high molar absorption near the UV/visible spectrum. These compounds have distinct advantages of absorbing in the near UV range where they bleach upon irradiation to generate benzoyl and phosphinoyl radicals. Both these free radicals proved to be very reactive (Decker *et al.*, 2001) and

capable to initiate the polymerization of a large variety of monomer such as acrylates, styrene, thiol-ene systems and maleimides (Dietliker, 1991). These compounds show a low volatility, as required for UV-curable water based systems, and UV powder, and a good solubility in acrylate monomers in particular the monoacylphosphine oxides (Reich *et al.*, 2000).

Further features of acylphosphine oxides include no quenching by monomers, such as styrene and very little yellowing of the cured coatings. A relatively high inhibition by oxygen may be troublesome in the curing of thin films. The absorption characteristic of acylphosphine oxides differ from most other photoinitiators of α -cleavage type in that they show enhanced absorption in the near UV/visible range (Reich *et al.*, 2000)..

These compounds have absorption maxima around 350 to 380 nm tailing to about 420 nm (Dietliker, 1991). Their long wavelength absorption and the bleaching effect make these initiators especially suitable for applications such as the curing of glass fibre reinforced polyester laminates, where relatively thick layers (up to 20 mm) of a material with reduced transparency (light absorption by the glass and scattering at the glass/resin interface) are to be polymerized.

The long wavelength absorption was identified as an $n \rightarrow \pi^*$ transition which is red-shifted as a result of a moderately strong conjugation between the phosphonyl group and the carbon atom to the adjacent carbonyl group. A similar red-shift observed in the UV spectra of acylphosphonates was explained by an overlap of the π -orbital on the carbonyl carbon atom with an empty d orbital on phosphorous.